























## Figure 1

(a) Schematics of our custom-made sample holder for the transfer of microscopic grains under  $N_2$  atmosphere ; (b) Sample transfer setup.

## Figure 2

(a) Ryugu mm-size grain A0064, (b) seven microscopic grains picked from A0064 stone, resting on the gold mirror of sample holder #3, (c) visible image of one of the picked grains, A0064-F0023, (d) SEM image of A0064-F0023 (HV 2 kV - 50 pA - ICE detector)



### Figure 3

SH3/A0064-FO020 in closed sample holder (through KBr window) (a) Optical image, (b) 2.7  $\mu\text{m}$  feature (hydration feature) band area integrated on hyperspectral image from MCT/A detector with synchrotron source, (c) SEM image of the grain taken after having opened the sample-holder Ryugu mm-size grain A0064, (d) spectra centered on the 2.7  $\mu\text{m}$  hydration feature of the selected grain, acquired through the KBr window.

(a) Near- and Mid-IR setup : Continuum microscope, FTIR spectrometer (Thermo Fisher) with MCT/B detector



(b) Mid-IR setup : Agilent Cary 670/620 microspectrometer with FPA array



(c) Far-IR setup : NicPlan microscope, IS50 FTIR spectrometer (Thermo Fisher) and bolometer detector (Infrared Laboratories)



**Figure 4**

The different systems used and their respective spectral ranges

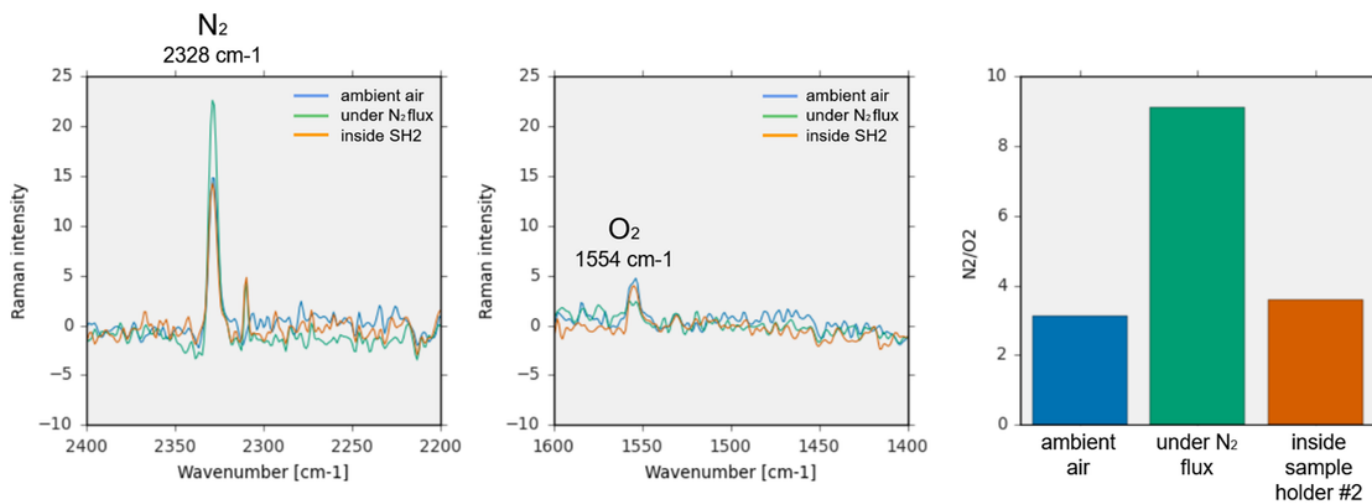


**Figure 5**

Raman spectra on SH2, detecting presence of both  $N_2$  and  $O_2$  inside, with an  $N_2/O_2$  ratio similar to that of ambient atmosphere

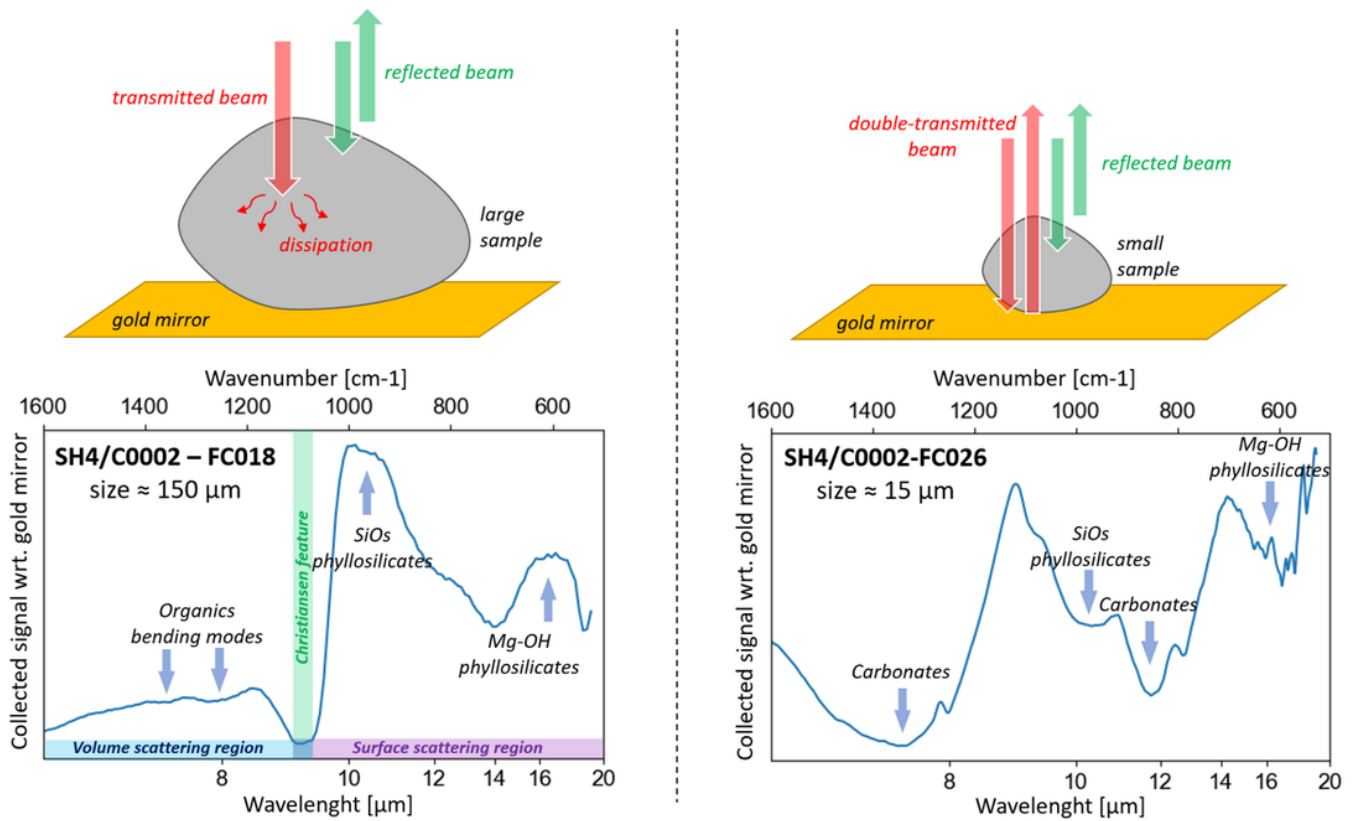


**Figure 6**

[left panel] cartoon modeling large grain behavior for infrared measurements on gold ; in the bottom panel, the collected signal with respect to a gold background from C0002-FC018, the largest grain in our set (size of approximately  $150 \mu\text{m}$ ). The collected signal behaves as expected from a standard reflectance measurement (spectral bands point downward before the Christiansen feature and upward after). [right panel] cartoon modeling large grain behavior for infrared measurements on gold, highlighting the contribution of a double-transmitted beam going through the sample and shining back towards the detector ; in the bottom panel, the collected signal with respect to a gold background from C0002-FC026, one of the smaller grains in our set (size of approximately  $15 \mu\text{m}$ ). The collected signal behaves erratically, with all the bands pointing downwards. The collected signal behaves like a transmission spectrum, even though it has been acquired in a reflectance configuration.

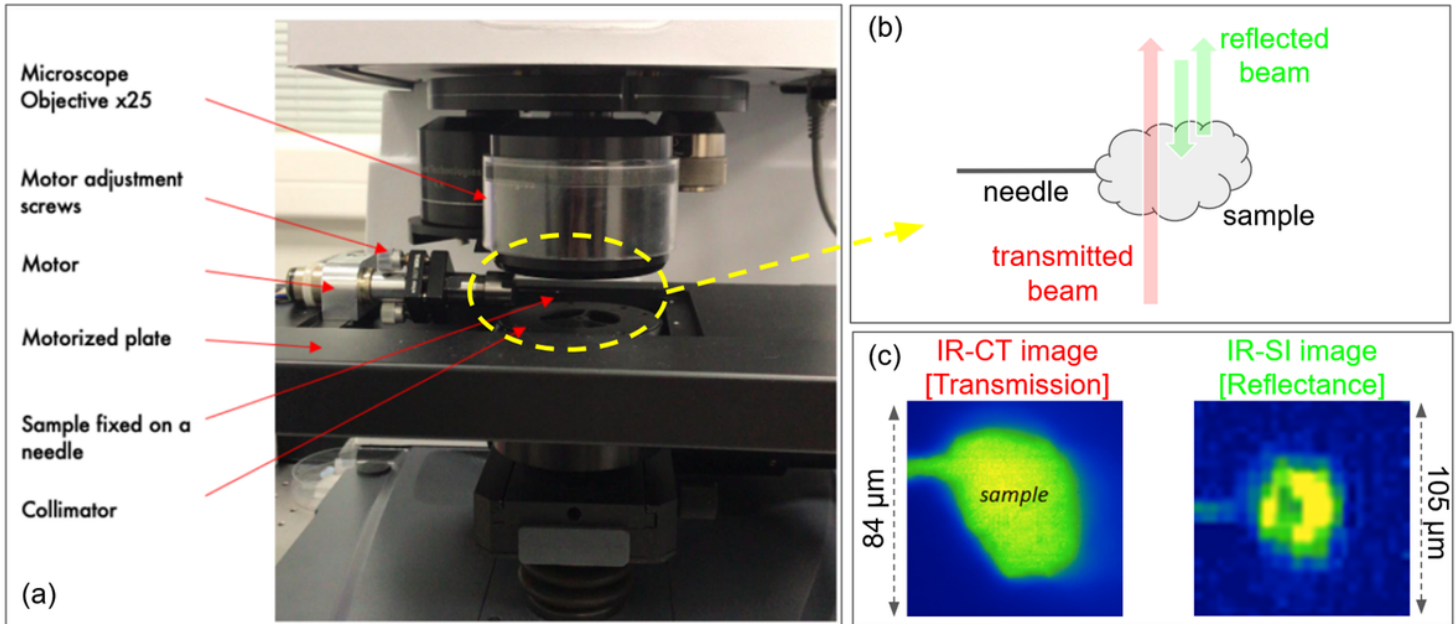


**Figure 7**

IR-CT and IR-SI principle of measurement. (a) description of 3D measurements setup pieces, (b) schematization of beam path for IR-CT measurements (transmitted beam) and IR-SI (reflected beam), (c) example of 1 hyperspectral image from IR-CT and IR-SI imaging techniques. The images shown in panel (c) correspond to the continuum signal at  $2.7 \mu\text{m}$  transmitted (for IR-CT) or reflected (for IR-SI) by the sample. For IR-CT, 90 images are acquired, one every  $2^\circ$ , rotating the sample from  $0^\circ$  to  $180^\circ$  : the final dataset consists of  $128 \times 128 \times 90$  spectels (a spectel is the equivalent of a pixel for hyper-spectral imaging : only one value can be associated to a pixel, while a whole spectra can be associated to a spectel). For IR-SI, 18 images are acquired, one every  $20^\circ$ , rotating the sample from  $0^\circ$  to  $360^\circ$  : the final dataset consists of  $32 \times 32 \times 18$  spectels.

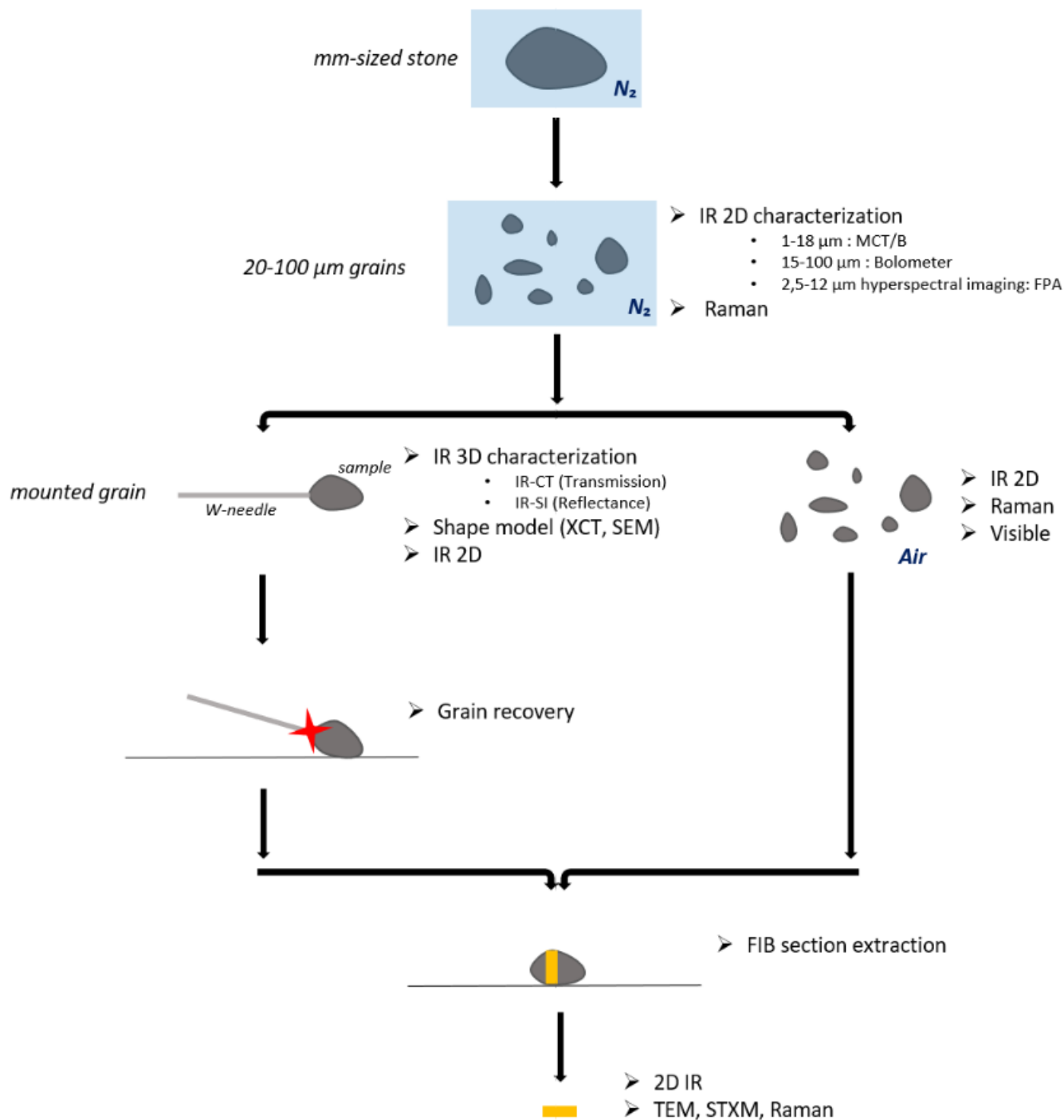


**Figure 8**

Cartoon summarizing the analytical pipeline used for Ryugu's particles. Note that everything is stored under a dry  $N_2$  atmosphere when not in this pipeline.

## Supplementary Files



This is a list of supplementary files associated with this preprint. Click to download.

- [graphicalabstractRubinoTechRep.png](#)